SAINT MARY'S UNIVERSITY SINCE 1802

The Secular Evolution of a Close Ring–Satellite System

Joseph M. Hahn
Saint Mary's University
Institute for Computational Astrophysics

Institute for Computational Astrophysics ICA

Introduction

Secular gravitational perturbations can play a significant role in determining the global structure and long-term evolution of a disk-companion system. The circumstellar dust-disk at β Pictoris is a well-known example, since its broad warp is thought to be due to secular perturbations exerted by an unseen planetary system (Mouillet et al 1997). Eccentric planets can make a dust-disk appear lopsided (Wyatt et al 1999), and inclined planets can also warp a more massive circumstellar gas disk, too (Lubow & Ogilvie 2001). And if that planet inhabits a gap in the gas disk, then its secular perturbations can launch spiral density waves at the gap edge (Goldreich & Sari 2003). But if the disk is instead gravity–dominated, then the companion can launch spiral density and bending waves at its secular resonances in the disk, which also tends to damp the companion's eccentricity and inclination (Ward & Hahn 1998, 2003).

The following will examine the secular evolution of a related system: of a small satellite that inhabits a narrow gap in a broad planetary ring, both of which are orbiting an oblate central planet. In particular, we will examine the spiral waves that the satellite can launch at the nearby ring edge, and will also examine how this wave–action tends to damp the satellite's eccentricity and inclination.

The rings model

The rings model of Hahn (2003) will be used to simulate the secular evolution of a ring–satellite system. The model treats the disk as a set of N nested, gravitating ellipses of mass m_j whose orientations are described by the usual orbit elements $a_j, e_j, i_j, \Omega_j, \tilde{\omega}_j$ and thickness h_j. The satellite is similarly represented here by a thin inclined ellipse. Because the masses of all perturbing bodies are smeared out over their orbits, this means that the model tracks the system's response to secular perturbations only. This also means that all other short-period perturbations are ignored: Lindblad resonances, most vertical resonances, and synodic impulses that produce wakes at the gap edges.

The system's evolution is described by the Lagrange planetary equations, and their solution is the familiar one for the secular evolution of N planets (Brouwer & Clemence 1961), except that the usual Laplace coefficients are softened by the ring's fractional thickness h/a (e.g., Hahn 2003).

Pan and the Encke gap

The rings model is used to simulate the spiral waves that Pan can launch in Saturn's rings. Pan is a 25km satellite that orbits in the 300 km–wide Encke gap in Saturn's main A ring. Figure 1 shows the eccentricities that are associated with the spiral density wave that Pan's secular perturbations launches at the outer edge of the Encke gap. A plot of the rings' inclinations (not shown) is similar.

Figure 2 shows the ring's longitudes $\tilde{\omega}$ and Ω versus semimajor axis a. Note that these longitudes rotate steadily with a, which indicates that these disturbances are indeed spiral density and spiral bending waves.

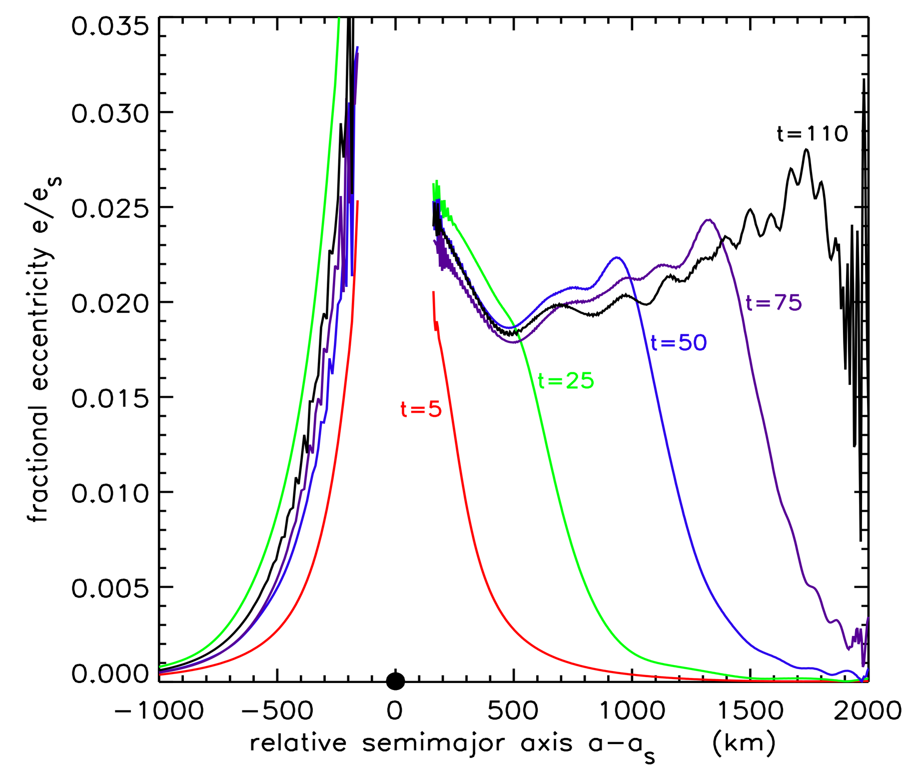

FIGURE 1: *Pan launches a density wave at the outer edge of the Encke gap.* Shown are the ring eccentricities e/e_S associate with this wave, plotted versus $a - a_s$ (radial distance from Pan) at selected times t (in years), where $e_S = 3.5\times10^{-5}$ is Pan's eccentricity (Spitale et al 2006). Other system parameters are: Pan's mass $\mu_s = 8.7\times10^{-12}$ in units of Saturn's mass M_1 (Porco et al 2005), the A ring surface density $\sigma = 50$ gm/cm^2 (Rosen et al 1991), so–called normalized disk mass $\mu_d = \pi\sigma a^2/M_1 = 5\times10^{-8}$, the Encke gap's fractional half–width $\Delta = 160$ km, and Saturn's second zonal harmonic $J_2 = 0.0163$.

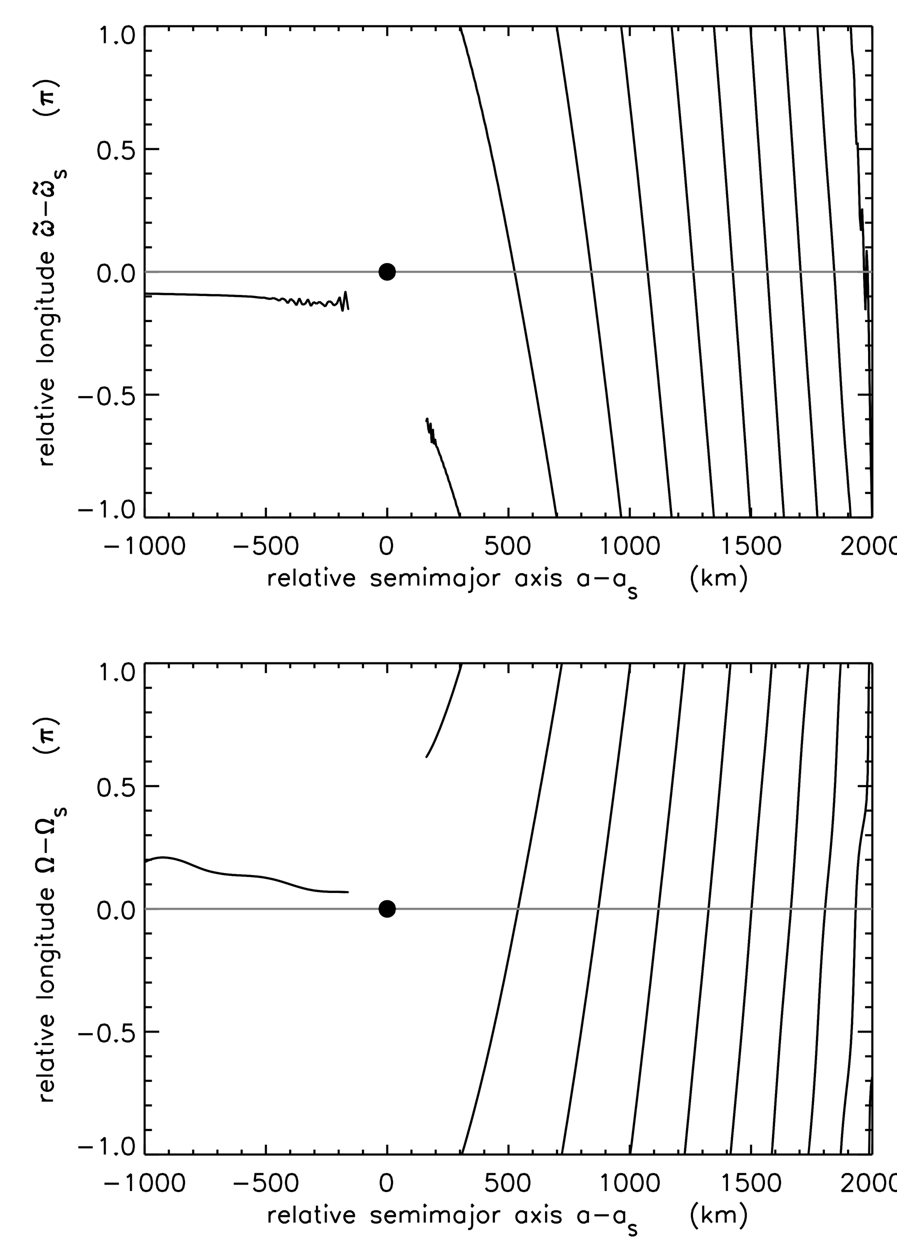

FIGURE 2: Upper figure shows the rings' longitudes of periapse $\tilde{\omega}$ relative to the satellite's longitude $\tilde{\omega}_s$. These curves represent an $m = 1$ armed trailing spiral density wave that slowly rotates at the rate $\dot{\tilde{\omega}}_s$, which is the satellite's apse precession rate. Maxima in the rings' surface density are 90° behind the $\tilde{\omega}$ curve. The lower figure shows the ring's longitudes of ascending node Ω relative to the satellite's node Ω_s. This is a one–armed spiral bending wave, and it rotates in a retrograde sense at the the satellite's precession rate $\dot{\Omega}_s$. Maxima in the ring plane's vertical displacement occur 90° ahead of Ω.

Horizontal & vertical displacements

The waves that Pan can launch at the Encke gap edge are actually rather modest disturbances in the A ring. Figure 3 shows the fractional variation in the ring's surface density due to Pan's density edge–wave, which is only $\Delta\sigma/\sigma \sim 0.5\%$. The initial wavelength is quite long, though, $\lambda \sim 500$km, and gets shorter further downstream.

The ring's vertical displacement due to the spiral bending wave launched at the gap edge depends on Pan's inclination. Spitale et al (2006) report an upper limit of $i = 0.001^\circ$ on Pan's inclination. Adopting this upper limit means the ring's vertical displacement is $z \lesssim 40$m (lower Fig. 3) due to the spiral bending wave launched at the gap edge, which is at most ~ 4 times the A ring's vertical thickness.

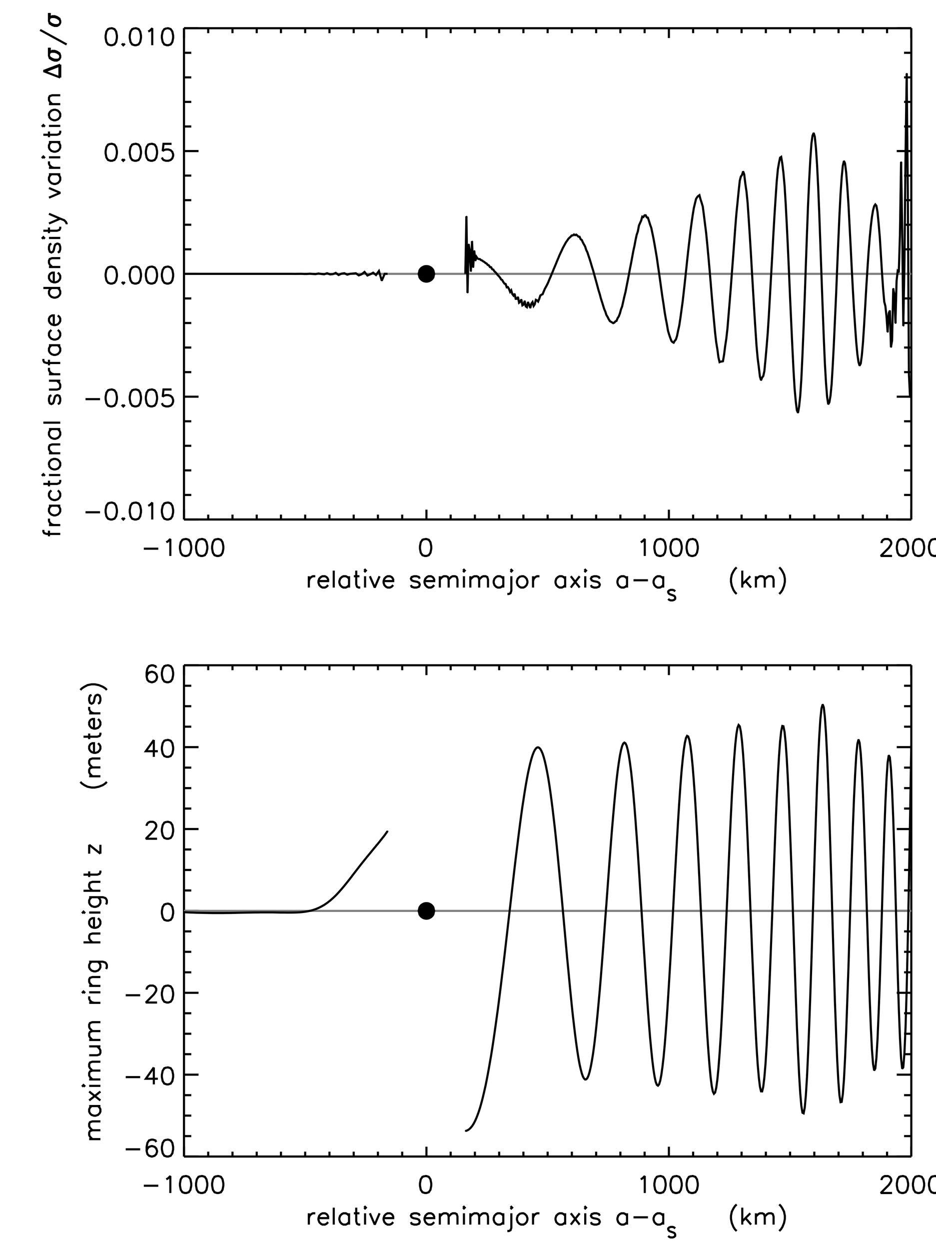

FIGURE 3: The ring's fractional surface density variations due to a spiral density wave is calculated from ring orbit elements via $\Delta\sigma/\sigma = eak\sin(\theta - \tilde{\omega})$ where $k = \partial\tilde{\omega}/\partial a$ is the wavenumber and θ is the longitude in the disk (Borderies et al 1985, Hahn 2003). The rings' maximal vertical displacement due to the spiral bending wave is $z = a\sin i\sin(\theta - \omega)$ assuming $i_s = 0.001^\circ$, which is the upper limit on Pan's inclination (Spitale et al 2006).

Eccentricity and inclination damping

The excitation of these spiral density and bending waves transfers angular momentum between the satellite and the nearby rings, which in turn damps the satellite's eccentricity e and inclination i; see Fig. 4. This is important since the fate of the satellite's e and i are somewhat uncertain.

Goldreich & Tremaine (1980) show that the satellite's corotation resonances in the ring tend to damp the satellite's e, while its Lindblad resonances excites e. And as long as the corotation resonances are unsaturated, e–damping is certain. But if that is not the case, then the Lindblad resonances will pump up the satellite's e over an e–fold timescale $\tau_e \simeq 10\Delta^4 P_{orb}/\mu_s\mu_d \sim 10^5$yrs. Pan's external vertical resonances in the ring also pump up its inclination over a comparable timescale (Borderies et al 1984, Ward & Hahn 2003).

However, Fig. 4 shows that the secular interactions damps Pan e's and i's at rates that are 40 times faster than the excitation due to Lindblad/vertical resonances. We suspect that these secular perturbations are responsible for circularizing Pan's orbit and confining it to the ring plane.

Wave reflection, and standing waves

But if these spiral waves fail to damp downstream, they will reflect at the ring's outer boundary and return to the launch site. The upper Fig. 5 shows that when the outward–bound *long, trailing* spiral density wave reflects at the ring's outer edge, it returns as a *short, leading* density wave, a phenomenon also seen in Hahn (2003).

And if the long, leading spiral bending wave reflects at the outer ring edge, it returns as a long trailing wave; see lower Fig. 5. The superposition of the two wavetrains results in a standing wave, one where the nodes alternate 180° every half–wavelength.

If reflected waves do manage to return to the vicinity of the satellite, they will communicate some of their angular momentum back into the satellite's orbit, which then stalls further eccentricity or inclination damping.

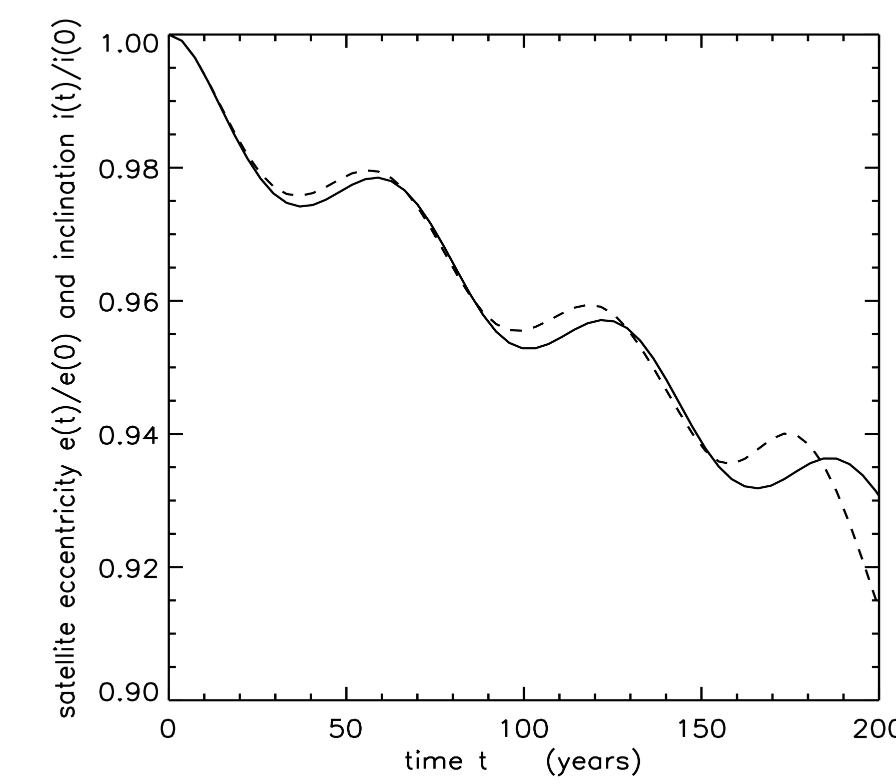

FIGURE 4: Pan's eccentricity $e(t)/e(0)$ and inclination $i(t)/i(0)$ plotted versus time t. Oscillations are due to Pan's secular interactions with the inner disk (which is itself a bit wobbly), while the steady decay is due to the excitation of spiral waves at the gap's outer edge. The orbit decay timescale for this secular damping of Pan's e's and i's is $\tau_s \sim 2500$ yrs.

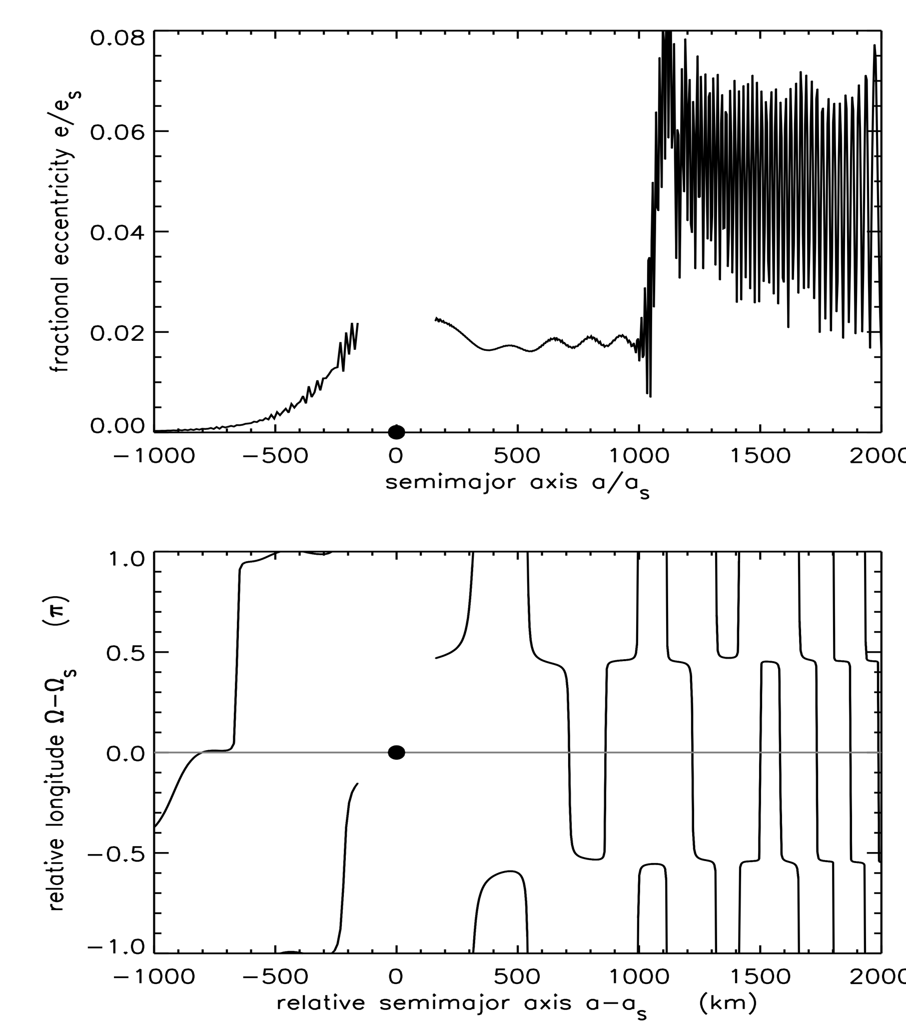

FIGURE 5: If spiral waves do not damp downstream, they reflect at the ring's outer edge. Upper figure shows an outward–bound, long, trailing density wave having $e \sim 0.02$ superimposed with a short, leading wave (the high–frequency wiggles) that reflected at the ring's outer edge. Lower figure shows the standing wave that results when the bending wave reflects at the ring's outer edge.

Towards an analytic theory

Lastly, the Lagrange planetary equations will be used to derive analytically the numerical results presented here. Our goal is to use those equations to derive the amplitude of these spiral density and bending waves, their dispersion relations, and the rates at which this wave-action damps the satellites eccentricity and inclination.